Int. J. Therm. Sci. (2000) 39, 909–918

S1290-0729(00)01188-1/FLA

An onset of nucleate boiling criterion for horizontal flow boiling

Olivier Zürcher [a], John R. Thome [b], Daniel Favrat [a]*

[a] *Laboratoire d'énergétique industrielle, Département de génie mécanique, École Polytechnique Fédérale de Lausanne LENI-DGM-EPFL, CH-1015 Lausanne, Switzerland*

[b] *Laboratoire de transfert de chaleur et de masse, Département de génie mécanique, École Polytechnique Fédérale de Lausanne, LTCM-DGM-EPFL, CH-1015 Lausanne, Switzerland*

(Received 17 April 2000, accepted 24 July 2000)

Abstract — A model to predict the onset of nucleate boiling has been successfully developed to differentiate purely convective evaporation from mixed nucleate and convective boiling during evaporation inside a horizontal tube of 14 mm I.D. Based on an extensive database collected for the natural refrigerant ammonia (R-717) over mass velocities from 10 to 140 $kg{\cdot}m^{-2}{\cdot}s^{-1}$, the analysis of the stratified, stratified-wavy and mainly annular flow patterns during evaporation with different heat flux ranges showed very accurate predictions in terms of the local heat transfer coefficient using this new onset of nucleate boiling criterion. © 2000 Éditions scientifiques et médicales Elsevier SAS

evaporation / local heat transfer coefficient / convection / nucleation / ammonia / substitute refrigerants

Nomenclature

A	cross sectional area	m^2
C_0	distribution factor	
c_0	distribution factor multiplier	
D	diameter	m
D_h	hydraulic diameter	m
d	vapor core diameter	m
G	mass velocity	$kg{\cdot}m^{-2}{\cdot}s^{-1}$
Δh_{evap}	latent heat	$J{\cdot}kg^{-1}$
h	heat transfer coefficient	$W{\cdot}m^{-2}{\cdot}K^{-1}$
h_L	liquid height in the tube	m
$\underline{M}$	molecular weight	$kg{\cdot}kmol^{-1}$
P	pressure	Pa
Pr	Prandtl number	
$\dot{q}$	heat flux	$W{\cdot}m^{-2}$
Re	Reynolds number	
r	radius	m
S	contact perimeter	m
T	temperature	K
u	velocity	$m{\cdot}s^{-1}$
V	drift velocity	$m{\cdot}s^{-1}$
x	vapor quality	
X_{tt}	Martinelli parameter	

Greek symbols

α	void fraction	
δ	liquid layer thickness	m
θ_{dry}	dry angle	rad
θ_{wet}	wetted angle	rad
λ	thermal conductivity	$W{\cdot}m^{-1}{\cdot}K^{-1}$
μ	dynamic viscosity	Pa·s
ξ	stratified–wavy angle	rad
ρ	density	$kg{\cdot}m^{-3}$
σ	surface tension	$N{\cdot}m^{-1}$
φ	stratified–wavy opening angle	rad
ψ	stratified–wavy wetting angle	rad

Subscripts

A	annular
cb	convective boiling
crit	critical
dry	dry
i	interface
L	liquid
nb	nucleate boiling

* Correspondence and reprints.
Daniel.Favrat@epfl.ch

ONB	onset of nucleate boiling
sat	saturation
Strat	stratified
Wavy	stratified–wavy
tp	two-phase
V	vapor
wet	wetted

1. RANGE OF APPLICATION AND STATE-OF-THE-ART

The substitution of CFC refrigerants in refrigeration systems, heat pumps and organic Rankine cycles requires good knowledge of the heat transfer performance of substitute fluids. A contribution to this international effort has been undertaken with this study on the natural refrigerant ammonia (R-717) for evaporation inside a single horizontal tube, in which the ammonia is heated by countercurrent flow of water in the annulus of the double-pipe type of test section. This is more appropriate than electrical heating for measuring local flow boiling heat transfer coefficients in stratified types of flow and also at high vapor qualities where part of the annular liquid film has dried out. The global conditions for ammonia were a saturation temperature of 4 °C, a heat flux range of 5–70 $kW{\cdot}m^{-2}$ and eleven mass velocities of $G = 10$, 20, 30, 40, 45, 50, 55, 60, 80, 120, 140 $kg{\cdot}m^{-2}{\cdot}s^{-1}$, corresponding to stratified, stratified–wavy, intermittent and annular flow patterns. The flow patterns were observed through tubular glass sections at both ends of the 3.1 m long test section. The heat transfer tube has an internal diameter of 14.00 mm, an external diameter of 15.86 mm and is made from a section of welded stainless steel type 439 tubing. Its thermal conductivity is 28 $W{\cdot}m^{-1}{\cdot}K^{-1}$.

The local heat transfer measurements were obtained from local heat fluxes and wall superheats. The local wall temperatures were determined from the mean value of four wall thermocouples installed in the wall at two different axial locations along the test section (adjusted to the inner tube wall temperature using Fourier's heat conduction law). The local saturation temperature was obtained from the vapor pressure curve of pure ammonia and the local saturation pressure, which was determined from a linear interpolation between the measured inlet and outlet pressures. The local heat fluxes were calculated from the slope of splines fit to the enthalpy profiles of the heating water flowing countercurrently in the annulus based on the water-side temperature measurements (four locations with four thermocouples at each location) such that local heat transfer coefficients could be measured similar to electrically heated test sections. Also using the enthalpy profile of water and an energy balance, the vapor quality of the refrigerant can be determined at each of the two wall thermocouple locations. *Figure 1* depicts a simplified diagram of the test loop.

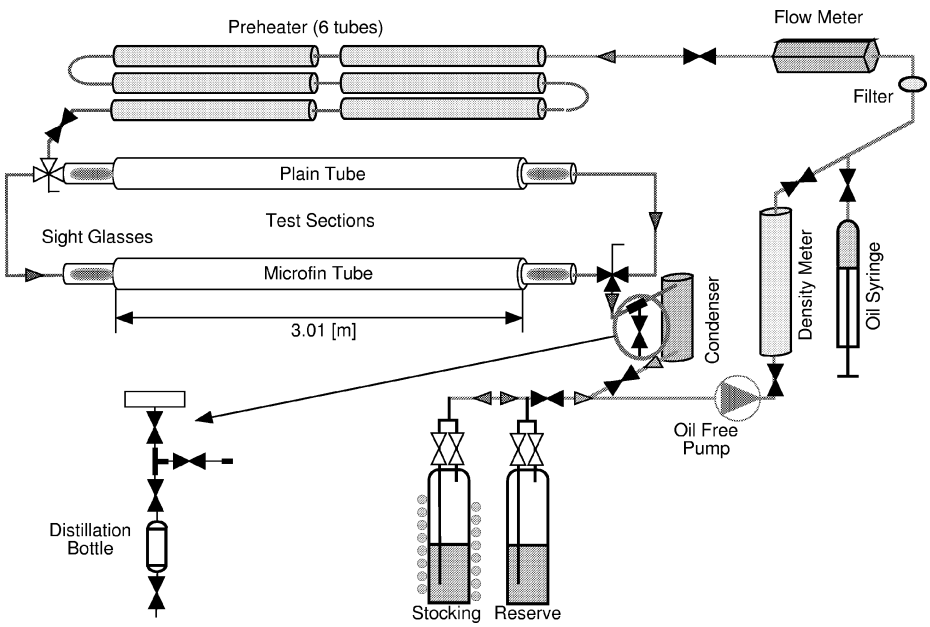

Figure 1. Simplified diagram of ammonia flow loop.

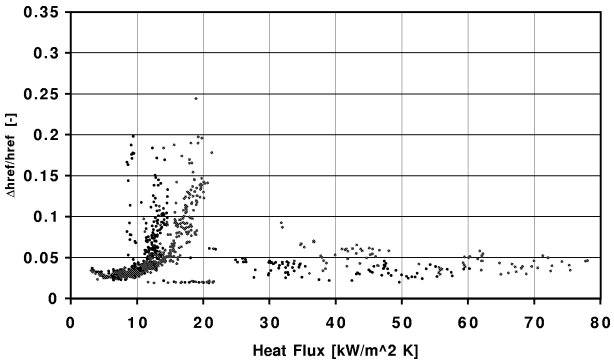

Figure 2. Relative uncertainity for the heat transfer coefficient as a function of heat flux.

Additional information about the experimental setup are available in Zürcher et al. [1] and more detailed information can be found in Zürcher [2]. The results of a propagation of error analysis is shown in *figure 2*.

The experimental heat transfer coefficients of ammonia were influenced by heat flux only in some vapor quality ranges and for some flow pattern types. Based on the geometrical approach originally proposed by Kattan et al. [3, 4] including the prediction of flow pattern, a new method has been developed in Zürcher [2] to predict the onset of nucleate boiling, which differentiates pure convective evaporation from combined nucleate and convective boiling.

Kattan et al. [3, 4] showed that even if different heat transfer models exist, such as the superposition, the enhancement and the asymptotic models, their range of reliable application is quite limited. They based this conclusion on a comprehensive database for fluorocarbon refrigerants covering different flow patterns and established that only heat transfer relations based on local flow pattern should today be seriously considered. However, even if the geometrical two-phase flow model that they proposed gave very accurate results in the annular and in the intermittent flow regions, it still suffered some weakness in the stratified and stratified–wavy regions, even if their method was still several times more precise than any of the other approaches tested. The large database, obtained presently for ammonia at low mass velocities and object of this paper, shows an important influence of heat flux on heat transfer in the stratified and stratified–wavy flow regimes, while no major influence is detected at higher mass velocities in the annular flow region.

The flow pattern proposed by Kattan et al. [3] is an improvement of the flow map of Steiner [5] for HFC refrigerants where the liquid level in a stratified configuration is calculated as part of the method. Due to the geometrical properties of the stratified configuration, this liquid level constitutes by consequence a void fraction. Assuming simplified relationships allowing an error of 1.5 % for the expressions of cross-sectional areas, Steiner used the assumption of identical pressure gradients for both separated phases of the stratified flow pattern domain to obtain a void fraction solution, which is similar to the earlier work of Taitel and Dukler [6]. The heat transfer prediction of Kattan et al. [4] is then based on a specific version for horizontal flow of the original void fraction model of Rouhani [7] proposed in [5]. Thus, two different void fraction models are used for identical conditions for the prediction of the flow pattern and the prediction of the heat transfer coefficient, which is not completely coherent.

If the flow pattern map model proposed by Kattan et al. [3] is very accurate for the five HFC refrigerants in their database, an empirical modification was proposed by Zürcher et al. [1] to better predict the ammonia flow patterns experimentally observed, and some further improvements were proposed in [2] to allow a more general flow pattern prediction of both fluorocarbon refrigerants (like HFC-134a and HFC-407C) and of the natural refrigerant ammonia.

The new unified method for the prediction of the local heat transfer coefficient during evaporation is proposed in [2]. This paper focuses on a new step in this method, which is the prediction of the onset of nucleate boiling to distinguish between pure convective boiling and mixed nucleate and convective boiling two-phase flow. Thus, only the main heat transfer relations used in the prediction procedure will be given here and other publications about the flow pattern map and the local heat transfer coefficient models will be submitted later this year.

2. PROPERTIES OF EACH FLOW PATTERN

The stratified flow pattern (*figure 3*) is characterized by the separation of the liquid and vapor phases by a smooth interface. This flow pattern occurs at very low mass velocities when the Kelvin–Helmholtz instability criterion is counterbalanced by the viscous forces.

From a geometrical point of view, the stratified flow pattern is the best defined flow pattern as the void fraction is a direct function of the wetted angle:

$$\alpha = \frac{2\pi - \theta_{\text{wet}} + \sin\theta_{\text{wet}}}{2\pi} \qquad (1)$$

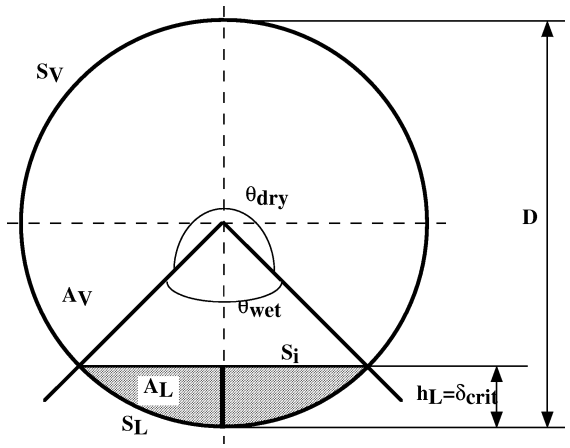

Figure 3. Cross-section of stratified configuration.

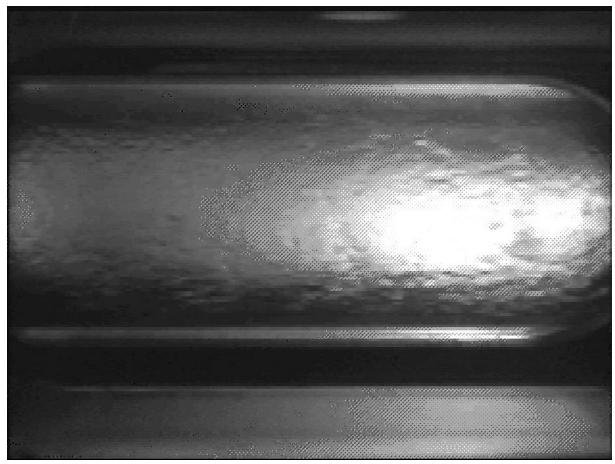

Figure 4. Annular flow pattern of pure ammonia flowing at $x = 81\,\%$ and $G = 122\ \mathrm{kg{\cdot}m^{-2}{\cdot}s^{-1}}$.

The precision of the void fraction model used will influence the liquid, the vapor and the interface velocities, but also the liquid height in the tube. As the liquid heat transfer coefficient is much larger than the vapor heat transfer coefficient, the liquid height is more important than the deviation of the velocities.

The annular flow pattern (*figure 4*) is obtained when the liquid wets all the tube periphery and the vapor flows at the center of the tube. Due to gravity, the film thickness is not constant around the periphery. The annular flow pattern has been considered to be reached as soon as the motion of the liquid flowing at the top of the tube was comparable to the one of the liquid at the bottom of the tube. Globally, the heat transfer coefficient for annular flows is characterized by a constant increase with increasing the vapor quality, until the breakup of the liquid film at the top of the tube occurs. At this point, the heat transfer coefficient reaches a peak and then decreases very rapidly towards the value of the all vapor heat transfer coefficient.

The annular flow pattern (*figure 5*), from a geometrical point of view and assuming no liquid entrainment in the vapor core, is fully determined with void fraction as long as the annular flow pattern is characterized by an all wetted perimeter and a circular vapor core of diameter d. The vapor core may either be centered or eccentric with respect to the central axis of the tube. The particular case where no liquid droplets are entrained in the vapor core is called the ideal annular configuration, where

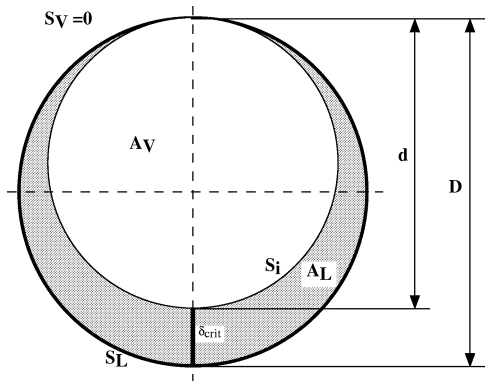

Figure 5. Cross-section of ideal annular configuration.

$$\alpha = \left(\frac{d}{D}\right)^2 \tag{2}$$

The stratified–wavy flow pattern (*figure 6*) is characterized by a wavy interface on the liquid. This flow pattern is a transitional one where waves exist but these are of a reduced magnitude and are not able to reach the top of the tube. In a cross-sectional view, the interface is curved (*figure 7*). Based on the heat transfer results where the general function of heat transfer is different for each flow pattern, the stratified–wavy region is considered to be a transition regime between the smooth interface region defined by the stratified flow pattern and the all-wetted and quite uniform mean distributed velocity in the liquid phase occurring for annular flow. Some flows that obviously wetted all the perimeter were found to be better described by the stratified–wavy model than the annular model when the liquid at the top of the tube was flowing very slowly, or at a noticeably different velocity than the liquid at the bottom of the tube.

The stratified–wavy flow pattern is more difficult to represent geometrically since the wetted angle is an independent variable. As shown in *figure 7*, the

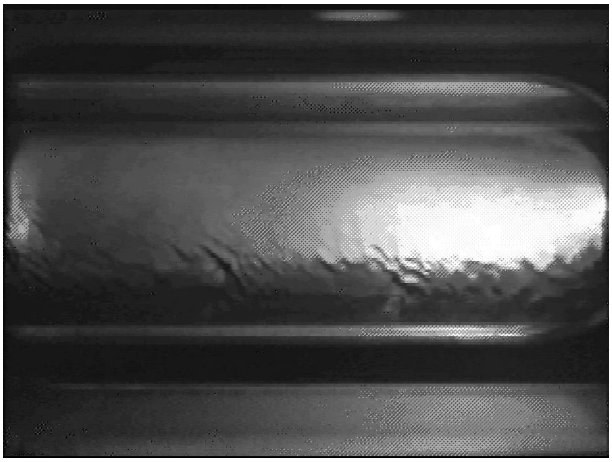

Figure 6. Stratified–wavy flow pattern of pure ammonia flowing at $x = 80\,\%$ and $G = 41$ kg·m^{-2}·s^{-1}.

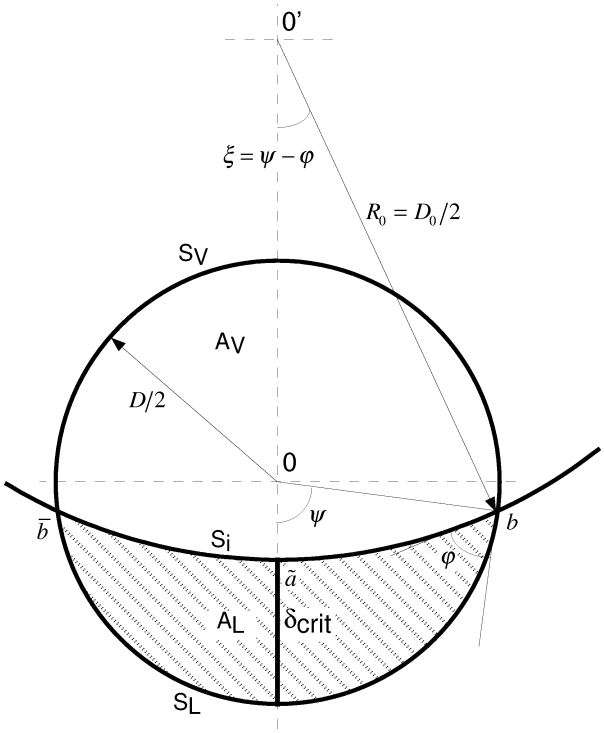

Figure 7. Modeling of the stratified–wavy flow pattern based on the intersection of two circles.

liquid cross-sectional surface can be modeled by the intersection of the inner tube wall and a second circle centered at 0′ with a radius of R_0. The parametrization of the circle is set as a function of two angles, called here the *half wetting angle* ψ and the *moon angle* φ. The difference between these two angles is called the *stratified–wavy angle* ξ. Void fraction is very important in the determination of the velocities of both phases and the location of the interface, which influence the convective heat transfer term; but the geometry of the stratified–wavy flow represented by the wetted angle also greatly influences the two-phase heat transfer coefficient. The void fraction corresponding to *figure 7* is

$$\alpha = 1 - \frac{1}{\pi}\left[\left(\psi - \frac{1}{2}\sin(2\psi)\right) - \frac{\sin^2\psi}{\sin^2\xi}\left(\xi - \frac{1}{2}\sin(2\xi)\right)\right] \tag{3}$$

3. VOID FRACTION MODELS

Zuber and Findlay [8] showed that void fraction is a parameter that depends on the flow properties, e.g., the velocity distribution. Thus, different void fraction models have been used, depending on flow pattern, for the prediction of the flow pattern map and the heat transfer coefficient in our new heat transfer model.

The separated flow model of Taitel and Dukler [6] has been used in the stratified flow region. Applied to a horizontal tube, the void fraction solution is obtained when

$$X_{tt}^2\left[\frac{(S_L)^{1.2}}{(1-\alpha)^3}\right] - \left[\frac{(S_V + S_i)^{0.2}}{\alpha^2}\left(\frac{S_V + S_i}{\alpha} + \frac{S_i}{1-\alpha}\right)\right] = 0 \tag{4}$$

where X_{tt} is the turbulent–turbulent Martinelli parameter and S is the contact perimeter (liquid to wall, vapor to wall and interface). As there is no particular advantage in the use of the nondimensional variables proposed by Taitel and Dukler [6], equation (4) is similar to the original expression for horizonal flow, but expressed in terms of void fraction and dimensional perimeters.

In the annular flow region, a void fraction model of Rouhani [7] has been used. Rouhani et al. [7] proposed a correlation based on the drift flux model of Zuber and Findlay [8] for vertical flow. Steiner in the VDI-Wärmeatlas [5] proposed a version of the Rouhani model applied to horizontal flow based on experimental data. The general expression of the drift flux model is

$$\alpha = \frac{x}{\rho_V}\left[C_0\left(\frac{x}{\rho_V} + \frac{1-x}{\rho_L}\right) + \frac{V_V}{G}\right]^{-1} \tag{5}$$

Steiner [5] proposed the following distribution parameter, based on a horizontal configuration in agreement with

experimental data:

$$C_0 = 1 + c_0(1 - x) \tag{6}$$

where $c_0 = 0.12$ and the weighted mean drift velocity of the vapor is

$$V_V = 1.18(1 - x)\left[\frac{\sigma g(\rho_L - \rho_V)}{\rho_L^2}\right]^{1/4} \tag{7}$$

The stratified–wavy flow is a central region between the stratified and the annular flow regions. The transition between the two flow pattern geometries is adapted with equation (5), where along the stratified–wavy to annular boundary the distribution parameter C_0 is based on Rouhani with $c_0 = 0.12$, and the needed C_0 to reproduce at a constant vapor quality, along the stratified to stratified–wavy boundary the void fraction obtained with the Taitel and Dukler [6] model. Into the stratified–wavy flow region, the value of c_0 is obtained by the linear interpolation of the respective values of c_0 along the two transition boundaries (stratified to stratified–wavy and stratified–wavy to annular) at a given vapor quality. While there is no physical justification for this interpolation, it allows a continuous void fraction solution across the transition boundaries, i.e. the evolution of the void fraction solution in the stratified-wavy flow region from a separated flow model (Taitel and Dukler) near the stratified flow region to a drift flux model (Rouhani) near the annular flow region.

With this, the stratified–wavy flow pattern will be treated with the drift flux model. This is motivated by the good agreement of this model to the two-phase situations where there is a notable interaction between the two phases. This is the case for annular flow and the stratified–wavy flow patterns, which tend to the annular flow configuration.

4. ONSET OF NUCLEATE BOILING CRITERION

Nucleate boiling is related to the nucleation of vapor bubbles in the liquid at the wall. This disturbes the liquid layer at the heated wall by the rapid growth of the bubbles. Due to the surface tension forces, a given amount of heat is needed for the onset of nucleate boiling. Steiner and Taborek [9] used the following criterion:

$$\dot{q}_{ONB} = \frac{2\sigma T_{sat} h_{cb,0}}{r_{crit}\rho_V \Delta h_{evap}} \tag{8}$$

where $r_{crit} = 0.3{\cdot}10^{-6}$ m is the critical bubble radius recommended for usual extruded tube materials and $h_{cb,0}$ is the *all liquid* convective heat transfer coefficient.

In pool boiling, the heat flux needed to activate boiling sites (defined in equation (8)) represents the required temperature difference for the onset of this phenomenon. Naturally, this onset value depends on the thermal resistance of the liquid layer, represented through the liquid convective heat transfer coefficient. Thus, because of the increases of the void fraction and the liquid mean velocity, the convective heat transfer coefficient $h_{cb,0}$ is not constant, and generally increases with increasing local vapor quality.

Prior flow boiling models combining the contribution of nucleate and convective boiling, such as Steiner and Taborek [9], are defined with the *all liquid* convective heat transfer coefficient. This *all liquid* convective coefficient is naturally calculated with the *all liquid* velocity and consequently with the tube diameter. Thus, the estimation of the temperature difference into the liquid layer is strongly overestimated as the vapor quality increases.

It is proposed here instead to define the onset of nucleate boiling (ONB) in two-phase flow with a more realistic convective heat transfer coefficient called the *critical convective heat transfer coefficient*. The idea is to consider that the heat transfer of the two-phase flow is only convective below ONB, and to define a critical heat flux value at which nucleation is activated. When the needed heat flux is obtained, the liquid heat transfer coefficient can be correlated with an asymptotic model.

Starting from the ONB criterion used by Steiner and Taborek [9] (equation (8)), a new relation for the minimum heat flux for the onset of nucleate boiling during evaporation is proposed to be

$$\dot{q}_{ONB,x} = \frac{2\sigma T_{sat} h_{cb,crit}}{r_{crit}\rho_V \Delta h_{evap}} \tag{9}$$

where $h_{cb,crit}$ is the convective heat transfer coefficient occurring during evaporation at the current vapor quality, and at the most advantageous location in the liquid cross section. As convective boiling is inversely proportional to the liquid thickness, the onset of nucleate pool boiling should occur at the location where the liquid thickness is the largest. Thus, the critical convective boiling heat transfer coefficient is defined as

$$h_{cb,crit} = C\, Re_\delta^m\, Pr_L^{0.4}\, \frac{\lambda_L}{\delta_{crit}} \tag{10}$$

where the values of the two constants $C = 0.01361$ and $m = 0.6965$ are based on experimental results of pure

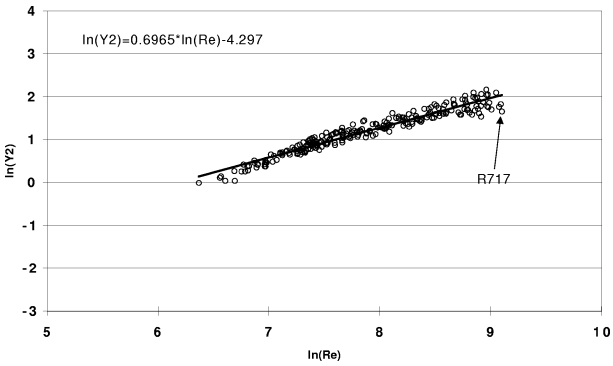

Figure 8. Determination of the leading constant C and the Reynolds number exponent m assuming pure convective heat transfer, based on ammonia measurements in annular flow.

convective heat transfer in annular flow (see *figure 8*). The film Reynolds number referred to a liquid layer is

$$Re_\delta = \frac{4\rho_L u_L \delta}{\mu_L} \tag{11}$$

Based on the geometrical representations of the flow patterns, the critical layer thickness applied to stratified flow (see *figure 3*) is

$$\delta_{\text{crit,Strat}} = \frac{D}{2}\left(1 - \cos\frac{\theta_{\text{wet}}}{2}\right) \tag{12}$$

For stratified–wavy flow pattern, the critical layer thickness is (see *figure 7*)

$$\delta_{\text{crit,Wavy}} = \frac{D}{2}\left(1 - \frac{\cos\psi + \cos\varphi}{1 + \cos(\psi - \varphi)}\right) \tag{13}$$

The annular flow liquid thickness varies between the mean film thickness and twice its value (see *figure 5*) as

$$\delta_{\text{crit,A}} = D - d = 2 \cdot \frac{D}{2}\left(1 - \sqrt{\alpha}\right) \tag{14}$$

Here twice the mean liquid layer is chosen as it corresponds to the thickest possible liquid layer in annular horizontal flow. It occurs along the stratified–wavy to annular flow transition and gives the smallest onset value. The ONB criterion is larger when the mean liquid thickness is considered at the bottom of the tube, but still with twice the liquid layer, the calculated ONB value was higher than most experimental heat fluxes.

Based on the present experimental database, good agreement has been obtained using a critical bubble radius in equation (9) of $r_{\text{crit}} = 0.38{\cdot}10^{-6}$ m (best fit with respect to the experimental data).

At the present experimental conditions, the ONB value is easily reached for stratified flow and sometimes for stratified–wavy flow, while no occurrence has been obtained for annular flow within the range of the heat fluxes tested.

5. EXPERIMENTAL RESULTS

In *figures 9* and *10*, a comparison is made between the experimental and the predicted heat transfer coefficients for pure ammonia at 4 °C in a smooth tube of 14 mm I.D. The experimental results are plotted as squares, and the predicted coefficients, calculated with the experimental conditions of each individual data point, are plotted as a bold line. The dashed line with triangles represents the ratio of the experimental heat flux to the ONB heat flux calculated with equation (9). Even if there is no physical meaning of the *line* between two calculated points, it helps to better visualize the relationship and improve readability. The data are for stratified and stratified–wavy flows at 20 $\text{kg}{\cdot}\text{m}^{-2}{\cdot}\text{s}^{-1}$ and for stratified–wavy and annular flows at 80 $\text{kg}{\cdot}\text{m}^{-2}{\cdot}\text{s}^{-1}$. The complete heat transfer calculation procedure cannot be detailed here, but will be later submitted to publication.

When the experimental heat flux is higher than the ONB heat flux value, the liquid heat transfer coefficient is calculated with the following asymptotic model. If the experimental heat flux is lower than the onset value, the nucleate boiling heat transfer coefficient h_{nb} is set to zero (pure convective heat transfer of the liquid):

$$h_{\text{wet}} = \left[(h_{\text{cb,L}})^3 + (h_{\text{nb}})^3\right]^{1/3} \tag{15}$$

where $h_{\text{cb,L}}$ is the liquid convective heat transfer coefficient calculated with the forced convection relation applied to a thin liquid layer:

$$h_{\text{cb,L}} = 0.01361 Re_\delta^{0.6965}\, Pr_L^{0.4}\, \frac{\lambda_L}{\delta} \tag{16}$$

and h_{nb} is the nucleate pool boiling heat transfer coefficient calculated with Cooper [10], which is

$$h_{\text{nb}} = 55\left(\frac{P}{P_{\text{crit}}}\right)^{0.12}\left[-\log\left(\frac{P}{P_{\text{crit}}}\right)\right]^{-0.55} \underline{M}^{-0.5}\dot{q}^{0.67} \tag{17}$$

The two-phase flow heat transfer coefficient is then obtained with

$$h_{\text{tp}} = \frac{\theta_{\text{dry}} h_V + (2\pi - \theta_{\text{dry}}) h_{\text{wet}}}{2\pi} \tag{18}$$

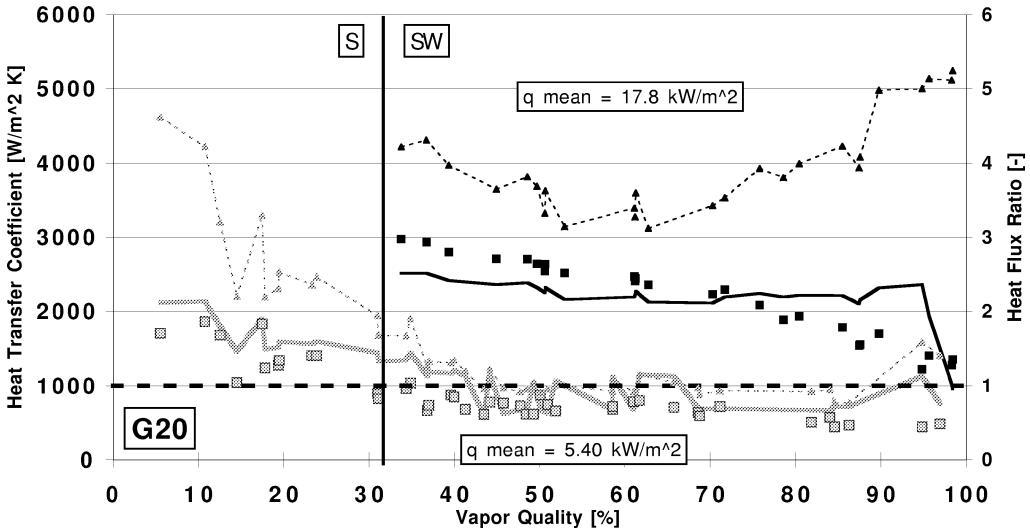

Figure 9. Comparison of experimental results (squares) to the new model (bold lines) of ammonia at $G = 20$ kg·m^{-2}·s^{-1}, and ratio of the experimental heat flux to the onset of nucleate boiling value (dashed lines).

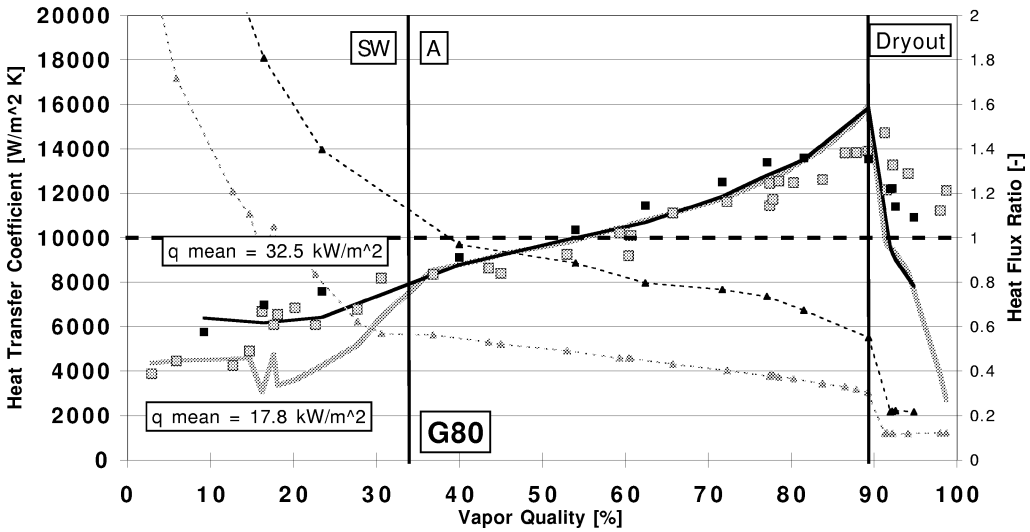

Figure 10. Comparison of experimental results (squares) to the new model (lines) of ammonia at $G = 80$ kg·m^{-2}·s^{-1}, and ratio of the experimental heat flux to the onset of nucleate boiling value (dashed lines).

where θ_{dry} is the angle measured from the center of the cross-section and expresses the angle occupied by the vapor phase while h_V is the convective vapor heat transfer coefficient calculated with the Dittus–Boelter correlation:

$$h_{cb,V} = 0.023 Re_{DV}^{0.8} Pr_V^{0.4} \frac{\lambda_V}{D} \qquad (19)$$

The term $(2\pi - \theta_{dry})$ in equation (18) represents the angle wetted by the liquid phase (see *figure 3*). This involves, of course, the knowledge of the geometrical distribution of both the liquid and vapor phases in the cross-section. Hence, use of a flow pattern map is imperative.

Figure 9 shows experimental and predicted heat transfer coefficients at $G = 20$ kg·m^{-2}·s^{-1} in a region with some pure stratified, but mainly with stratified–wavy flow patterns. The upper mean heat flux ($\dot{q} = 17.8$ kW·m^{-2}) has been treated over the full range with the asymptotic model which involves a nucleation boiling contribution. The mean heat flux was clearly higher than the onset

value obtained with equation (9) while for the lower heat flux ($\dot{q} = 5.40$ kW·m^{-2}) the mean heat flux applied on the liquid was of the same order of magnitude as the onset value. Due to the noncontinuous heat transfer prediction between the pure convective and the asymptotic models, some jumps appear in the prediction showing the intermittence of asymptotic and pure convective liquid heat transfer coefficients. Nevertheless, it must be noted that the upper and lower values of the jump still define clearly an accurate prediction.

The predictions for $G = 20$ kg·m^{-2}·s^{-1} involve the use of the stratified–wavy wetted angle. Even if this angle is still very close to the stratified one, the proposed prediction shows accurate results in a domain where the number of free parameters is the largest. It is also important to observe that the general tendency of the stratified–wavy heat transfer coefficient is a slow monotonic decrease during evaporation. Using the complete heat transfer procedure, the standard deviation of the tests at $G = 20$ kg·m^{-2}·s^{-1} is 33.4 % for the lower mean heat flux and 27.1 % for the larger mean heat flux. In contrast, the Gungor and Winterton (1987) flow boiling correlation with its stratification correction factor mispredicts these data by about a factor of 2 (see [1]).

Figure 10 shows complete evaporation at different heat flux ranges. The heat flux level was not high enough to reach the onset of nucleate boiling in the annular flow configuration. A few experimental points at high heat flux reached the onset value, but based on the experimental points, no specific enhancement of the heat transfer coefficient existed in our database. Due to this, the pure convective liquid coefficient has been applied to the full range of evaporation in annular flow. Remember also that the critical liquid height defined for annular flow is twice the liquid layer thickness. As the annular flow regime is well established, the cross-sectional geometry is better represented by a pure axisymmetric flow than an annular flow at the onset of dryout limit (refer to *figure 5*). Thus, the real heat flux needed for onset of nucleate boiling in annular flow has not been reached during these experiments, even if the ratio of the experimental heat flux to the onset of nucleate boiling value is close to one in *figure 10*.

This last remark is not to be considered in the other flow regimes. At a mean heat flux of $\dot{q} = 32.5$ kW·m^{-2}, the model uses the asymptotic approach in the stratified–wavy region, while a transition from asymptotic to pure convective is shown on the same graph at a mean heat flux of $\dot{q} = 17.8$ kW·m^{-2} at a vapor quality of $x = 18$ %. The standard deviation of the tests at $G = 80$ kg·m^{-2}·s^{-1} is 25.0 % for the lower mean heat flux and 12.9 % for the larger mean heat flux. Note that these standard deviations in annular flow are strongly affected by the data in the partial dryout region after the peak because of the rapid decrease of the heat transfer coefficient; before dryout the predictions are very precise.

6. CONCLUSION

A criterion to differentiate pure convective evaporation from combined nucleate and convective heat transfer during evaporation has been proposed. The approach of Steiner and Taborek [9] has been modified to include the real mean flow conditions of the liquid and a geometrical modelization of the liquid cross-section. It has been shown that the experimental influence of the heat flux on the local heat transfer coefficient has been accurately detected with the new onset of nucleate boiling criterion. Included in the complete procedure of heat transfer coefficient prediction, which is based on a flow map prediction, a mean weighted coefficient and an asymptotic model in the case of mixed convective and nucleate boiling heat transfer, the standard deviations of the proposed cases were all less than 35.0 %. These values overstate the actual deviations of the method since many data were purposely taken near flow regime transitions and at very high vapor qualities, which are the most difficult to predict.

Acknowledgements

This work has been carried out at the Laboratory for Industrial Energy Systems (LENI), Swiss Federal Institute of Technology in Lausanne (EPFL). The project has been supported financially by the EPFL, the Swiss Federal Office of Energy (OFEN) and Research grant 800-RP from the American Society of Heating, Refrigeration and Air-Conditioning Engineers (ASHRAE), which are gratefully acknowledged.

REFERENCES

[1] Zürcher O., Thome J.R., Favrat D., Evaporation of ammonia in a smooth horizontal tube: Heat transfer measurements and predictions, J. Heat Tran. 121 (1999) 89–101.

[2] Zürcher O., Contribution to the heat transfer analysis of natural and substitute refrigerants evaporated in a horizontal tube, Ph.D. thesis No. 2122, Swiss Federal Institute of Technology, Lausanne, 2000.

[3] Kattan N., Thome J.R., Favrat D., Flow boiling in horizontal tubes. Part 1: Development of a diabatic two-phase flow pattern map, J. Heat Tran. 120 (1998) 140–147.

[4] Kattan N., Thome J.R., Favrat D., Flow boiling in horizontal tubes. Part 3: Development of a new heat transfer model based on flow patterns, J. Heat Tran. 120 (1998) 156–165.

[5] VDI-Wärmeatlas (VDI Heat Atlas), Verein Deutscher Ingenieure, VDI-Gesellschaft Verfahrenstechnik und Chemieingenieurwesen (GCV), Düsseldorf, 1993, Chapter Hbb.

[6] Taitel Y., Dukler A.E., A model for predicting flow regime transitions in horizontal and near horizontal gas–liquid flow, AIChE J. 22 (1) (1976) 47–55.

[7] Rouhani S.Z., Axelsson E., Calculation of void volume fraction in the subcooled and quality boiling regions, Int. J. Heat Mass Tran. 13 (1970) 383–393.

[8] Zuber N., Findlay J.A., Average volumetric concentration in two-phase flow systems, J. Heat Tran. 87 (1965) 453–468.

[9] Steiner D., Taborek J., Flow boiling heat transfer in vertical tubes correlated by an asymptotic model, Heat Transfer Engineering 13 (2) (1992) 43–69.

[10] Cooper M.G., Saturation nucleate boiling: A simple correlation, in: The First UK National Conference on Heat Transfer, Vol. 2, 1984, pp. 785–793 (I. Chem. E. Symposium Series No. 86, 1984).

[11] Cooper M.G., Correlations for nucleate boiling — Formulation using reduced properties, Physicochem. Hydrodyn. 3 (1982) 89–11.

[12] VDI-Wärmeatlas (VDI Heat Atlas), Verein Deutscher Ingenieure, VDI-Gesellschaft Verfahrenstechnik und Chemieingenieurwesen (GCV), VDI Verlag, Düsseldorf, 1997, Chapter Ha.

[13] Stephan K., Abdelsalam M., Heat transfer correlations for natural convection boiling, Int. J. Heat Mass Tran. 23 (1980) 73–87.

[14] Zürcher O., Thome J.R., Favrat D., Development of a diabatic two-phase flow pattern map for horizontal flow boiling, to be submitted.

[15] Zürcher O., Thome J.R., Favrat D., Development of a new heat transfer model based on flow pattern for horizontal flow boiling, to be submitted.